Identification of the Ferroptosis-Related Long Non-Coding RNAs Signature to Improve the Prognosis Prediction in patients with NSCLC

Meng Li
Xi'an Jiaotong University Medical College First Affiliated Hospital
Yanpeng Zhang
Xi'an Jiaotong University Medical College First Affiliated Hospital
Meng Fan
Xi'an Jiaotong University Medical College First Affiliated Hospital
Hui Ren
Xi'an Jiaotong University Medical College First Affiliated Hospital
Mingwei Chen
Xi'an Jiaotong University Medical College First Affiliated Hospital
Puyu Shi (shipuyu@xjtufh.edu.cn)
Xi'an Jiaotong University Medical College First Affiliated Hospital https://orcid.org/0000-0002-3477-0148

Primary research

Keywords: non-small cell lung cancer, ferroptosis, long non-coding RNAs, prognostic, signature

Posted Date: June 15th, 2021

DOI: https://doi.org/10.21203/rs.3.rs-598005/v1

Abstract

Background: Non-small cell lung cancer (NSCLC) is the most prevalent type of lung carcinoma with an unfavorable prognosis. Ferroptosis, a novel iron-dependent programmed cell death, is involved in the development of multiple cancers. Of note, the prognostic value of ferroptosis-related lncRNAs in NSCLC remains uncertain.

Methods: Gene expression profiles and clinical information of NSCLC were retrieved from the TCGA database. Ferroptosis-related genes (FRGs) were explored in the FerrDb database and ferroptosis-related lncRNAs (FRGs-lncRNAs) were identified by the correlation analysis and the LncTarD database. Next, The differentially expressed FRGs-lncRNAs were screened and FRGs-lncRNAs associated with the prognosis were explored by univariate Cox regression analysis and Kaplan-Meier survival analysis. Then, an FRGs-lncRNAs signature was constructed by the Lasso-penalized Cox model in the training cohort and verified by internal and external validation. Finally, the potential correlation between risk score, immune response, and chemotherapeutic sensitivity was further investigated.

Results: 129 lncRNAs with a potential regulatory relationship with 59 differentially expressed FRGs were found in NSCLC and 10 FRGs-lncRNAs associated with the prognosis of NSCLC were identified (P<0.05). 9 prognostic-related FRGs-lncRNAs (AQP4-AS1, DANCR, LINC00460, LINC00892, LINC00996, MED4-AS1, SNHG7, UCA1, and WWC2-AS2) were used to construct the prognostic model and stratify patients with NSCLC into high- and low-risk groups. Kaplan-Meier analysis demonstrated a worse outcome in patients with high risk (P<0.05). Moreover, a good predictive capacity of this signature in predicting NSCLC prognosis was confirmed by the ROC curve analysis. Additionally, 45 immune checkpoint genes and 8 m6A-related genes were found differentially expressed in the two risk groups, and the sensitivity of 28 chemotherapeutics were identified to be correlated with the risk score.

Conclusion: A novel FRGs-lncRNAs signature was successfully constructed, which may contribute to improving the management strategies of NSCLC.

Introduction

Lung cancer ranks top in the incidence of malignancies and imposes an enormous socio-economic burden worldwide [1]. Non-small-cell lung cancer (NSCLC) is the most prevalent subtype of primary lung cancer, among which adenocarcinoma (LUAD) as well as squamous cell carcinoma (LUSC) are the leading histology[2, 3]. Although there have been breakthroughs in the targeted therapy and immunotherapy of lung cancer, the long-time survival rate of NSCLC remains unsatisfactory [4–6], and most patients will inevitably develop drug resistance. Since most anti-tumor drugs play a therapeutic role by inducing apoptosis of cancer cells, it is of great significance to pinpoint novel cell death pathways in NSCLC and discover new directions for identifying treatment strategies and evaluating prognosis.

Ferroptosis, a newly discovered mode of iron-dependent regulated cell death unlike apoptosis, pyroptosis, autophagy and necrosis, is mainly caused by the iron accumulation-mediated lipid peroxidation and

exhibits peculiar morphology, genetics, as well as biochemistry features [7]. The development of disease and organisms and anti-tumor drug resistance has also been verified to be affected by ferroptosis [8, 9]. Long non-coding RNAs (lncRNAs) is a kind of RNA with more than 200 bases in length. Although lncRNAs lack protein-coding ability, it is still considered a target for gene therapy of cancer since it is involved in the tumor occurrence, development as well as metastasis by modulating gene expression at chromatin, transcriptional, and post-transcriptional levels[10, 11]. Additionally, some lncRNAs were found to inhibit ferroptosis by acting as competitive endogenous RNA to prevent oxidation in various cancers including lung cancer. [12, 13]. Metallothionein 1D pseudogene, a lncRNA, was found to sensitize erastin-induced ferroptosis in NSCLC by modulating the miR-365a-3p/NRF2 axis [14]. A G3BP1-interacting lncRNA was demonstrated to promote ferroptosis via nuclear sequestration of p53 in lung carcinoma [15]. Whereas, the signature of ferroptosis-related lncRNAs and its association with prognosis in NSCLC has not been systematically evaluated.

Herein, we explored the expression of ferroptosis-related genes (FRGs) and ferroptosis-related lncRNAs (FRGs-lncRNAs) in NSCLC and further investigate the relationship between these lncRNAs and the prognosis in NSCLC based on the Cancer Genome Atlas (TCGA) database. Subsequently, a prognostic model was constructed on the basis of FRGs-lncRNAs in the training set and verified by internal and external validation. Furthermore, the relationship between risk score, clinicopathological features, immune responses, N6-methyladenosine (m6A) mRNA statues, and chemotherapeutics sensitivity was further elucidated in NSCLC.

Materials And Methods

Data acquisition and processing

Gene expression profiles and clinical features of TCGA-LUAD (510 tumors and 58 normal) and TCGA-LUSC (496 tumors and 49 normal) were obtained from UCSC Xena (https://xena.ucsc.edu/). The expression profiles of LUAD and LUSC were combined as NSCLC expression matrix, and a total of 1093 patients (986 tumors and 107 normal) were eventually included in the present study after the batch correction by using ComBat function of the R “sva” package. No ethics committee approval and informed consent of patients were required in this study since the data were obtained from a public database.

Identification of FRGs

259 FRGs (Table S1) were explored from the “Marker”, “Driver” and “Suppressor” modules of the FerrDb database (http://www.zhounan.org/ferrdb/) [16], among which 241 were found to be expressed in NSCLC. The expression profiles of these FRGs were extracted to identify the differentially expressed FRGs (DE-FRGs) between normal and tumor by the “limma” package of R. $|log2FC|>1$and $FDR < 0.05$ is considered to be significant.

Functional enrichment analysis

“ClusterProfiler” of R was utilized to conducted Gene Ontology (GO) as well as Kyoto Encyclopedia of Genes and Genomes (KEGG) analysis to investigate the biological functions and signaling pathways affected by these DE-FRGs [17].

Screening of FRG-lncRNAs

The Pearson correlation analysis was conducted to identify the potential lncRNAs correlated with DE-FRGs based on the TCGA database. |R|>0.5 and $P < 0.001$ were considered a strong correlation. In addition, the lncRNAs that have a regulatory relationship with DE-FRGs and expressed in NSCLC were further explored and screened in the LncTarD database (http://bio-bigdata.hrbmu.edu.cn/LncTarD/)[18]. Then, lncRNAs that have an expression and regulatory relationship with DE-FRGs in TCGA and LncTarD database were unionized to obtain candidate FRGs-lncRNAs. The “survival” package, univariate Cox regression analysis, and Kaplan–Meier (K-M) survival method were conducted to investigate FRGs-lncRNAs associated with the prognosis in NSCLC.

FRG-lncRNAs prognostic model construction

986 NSCLC patients were separated into a training set and verification set at a ratio of 7:3 by R randomly (690 and 296 patients in the training and test set, respectively). Lasso-penalized Cox regression analysis was performed to establish a FRGs-lncRNAs prognostic model in the training set using the R “glmnet” package [19, 20]. The risk score of each sample was calculated on the basis of the normalized expression levels and the corresponding Lasso’s coefficient of the FRGs-lncRNAs [Risk score=$\sum$exp(i)*coef(i)], and patients were further categorized as high- and low-risk groups in accordance with the median risk score. Then “ggplot2” package of R were performed to draw the survival scatter plot. K-M survival curve and receiver operational characteristic (ROC) curves were generated to evaluate the relationship between risk score and prognosis, and the predictive capacity of the signature. Additionally, the expression levels of FRGs-lncRNAs of each sample in the two risk groups were uncovered by “heatmap” package. Finally, the results were further identified in the internal and external validation groups.

Predictive nomogram construction

Wilcoxon test was performed to investigate the potential relationship between risk score and multiple clinical features (EGFR mutation, ALK-EML4 rearrangement, age, gender, stage, and TNM stage). $P < 0.05$ was considered to be significant. Subsequently, the independent prognostic factors were investigated by univariate and multivariate Cox regression analysis and visualized the results by R “forestplot” package. Finally, a nomogram was established integrating the clinical features and risk score for predicting 1, 3, and 5-year overall survival (OS) of NSCLC patients, and the prediction accuracy of which was further evaluated by the calibration and ROC curve.

Immunity analysis and gene expression

Five algorithms, ESTIMATE, ssGSEA, MCPcounter, TIMER and CIBERSORT were utilized to evaluate the correlation between risk score and the immune response in NSCLC, and the heatmaps were used to

uncover the differences of immune cell infiltration between the two risk groups under different algorithms.

Expression of immune checkpoint and m6A expression in NSCLC

79 immune checkpoint genes (ICGs) were explored from the literature (PMID: 32814346), of which 66 were expressed in NSCLC. Student t-test was used for difference analysis, and the top 10 ICGs with significant differences were shown as boxplots. In addition, the expression differences of the 13 factors involved in m6A between the high and low-risk groups were further analyzed.

Correlation analysis between risk score and chemotherapeutic drugs sensitivity

All the cell lines in the Cancer Genome Project (CGP) database [21] combined with the expression profile of the training set were utilized to evaluate the role of the risk score in the sensitivity of chemotherapeutics by using the R package “pRRophetic”. A total of 138 chemotherapeutics were identified in the CGP database, then, Pearson correlation analysis was performed to investigate the relationship between risk score and drug sensitivity. $P < 0.05$ and $|R| > 0.3$ is considered significant correlation.

Statistical analysis

Perl and R (4.0.1) were utilized for data processing and statistical analysis. Benjamini-Hochberg method was performed to identify the DE-FRGs. Pearson correlation analysis were conducted to explore the lncRNAs associated with DE-FRGs. FRGs-lncRNAs associated with prognosis were explored by univariate Cox regression tests and K-M survival analysis in NSCLC. A FRGs-lncRNAs prognostic model was generated by the Lasso-penalized Cox regression analysis and further evaluated the predictive capacity by K-M survival and ROC curve analysis. Independent predictors of OS in NSCLC were identified by multivariate Cox regression analysis. $P < 0.05$ was considered significant.

Results

Identification and enrichment analysis of FRGs in NSCLC

986 patients with NSCLC and 107 healthy control from the TCGA database were enrolled in the present study. 259 FRGs were explored from the FerrDb database, and 241 were found to be expressed in NSCLC (Table S1). The process of our research is shown in Fig. 1. Herein, we found 59 FRGs were significantly differentially expressed between normal and NSCLC patients (28 downregulated and 31 upregulated, Fig. 2A and B). The DE-FRGs were determined mainly involved in biological pathways related to the response to oxidative stress, lipid droplet, and oxidoreductase activity biological function by GO analysis

(Fig. 3A). KEGG enrichment analysis revealed that these DE-FRGs also participate in ferroptosis, arachidonic acid metabolism, glutathione metabolism, and NOD-like receptor signaling pathway (Fig. 3B).

Identification of the ferroptosis-related lncRNAs in NSCLC

104 FRGs-lncRNAs were identified by Pearson correlation analysis (|R| > 0.5, $P < 0.001$) and the top 10 of which were selected for further analysis (Fig. 4A). Next, 44 lncRNAs that have a regulatory relationship with DE-FRGs were explored in the LncTarD database, and 30 of them were determined to be expressed in NSCLC. The interaction network between DE-FRGs and lncRNAs were shown in Fig. 4B. Finally, 129 candidate FRGs-lncRNAs were collected in this study by unifying the lncRNAs that have an expression or regulatory relationship with DE-FRGs based on TCGA and LncTarD database (Fig. 4C, Table S2). Then, 13 FRGs-lncRNAs associated with NSCLC prognosis were identified by univariate Cox analysis ($P < 0.05$, Fig. 5A, Table S3), among which, 10 lncRNAs also showed significant results in K-M analysis and selected for the prognostic model construction (Table S4). The survival curves of the first 6 lncRNAs were demonstrated in Fig. 5B-G ($P < 0.05$).

Construction of the prognostic model based on ferroptosis-related lncRNAs

986 NSCLC patients were categorized into training and testing cohorts randomly at a ratio of 7:3, and 9 of the 10 prognostic FRGs-lncRNAs (AQP4-AS1, DANCR, LINC00460, LINC00892, LINC00996, MED4-AS1, SNHG7, UCA1, and WWC2-AS2) were eventually used for prognostic signature construction by Lasso-penalized Cox regression analysis (Fig. 6A and B, Table S5). Then, patients were classified into a high and low-risk group in accordance with the median of risk score [Risk score = exp(AQP4-AS1) * -0.268 + exp(DANCR) * -0.041 + exp(LINC00460) * 0.122 + exp(LINC00892) * -0.390 + exp(LINC00996) * -0.144 + exp(MED4-AS1) * -0.198 + exp(SNHG7) * -0.028 + exp(UCA1) * 0.092 + exp(WWC2-AS2) * 0.497] and patients with higher risk scores showed shorter survival time in the survival status plot (Fig. 6C and D). Additionally, the K-M plot illustrated a worse prognosis in the NSCLC patients with the high-risk (P 0.001, Figure E) and ROC curve analysis demonstrated AUC for predicting NSCLC prognosis were 0.606 (Fig. 6F). The expression levels of the 9 FRGs-lncRNAs in each sample between the two risk groups are presented in Fig. 6G.

Validation of the prognostic signature

To evaluate the robustness of the prognostic model, the patients from the testing cohort were also grouped according to the median of the same risk score (Fig. 7A), and patients with high risk were found to reach the end of life earlier like the training group (Fig. 7B). At the same time, a poor prognosis was found in NSCLC patients with high risk in the testing group simultaneously ($P = 0.004$, Fig. 7C), and a good accuracy of the prognostic model in predicting the OS of NSCLC were also elucidated in the testing group (Fig. 7D, AUC = 0.604). The expression trend of the 9 FRGs-LncRNAs between the two risk groups of the testing cohort was similar to that of the training group (Fig. 7E).

In addition, external validation was also carried out in GES31210 to further verify the effectiveness of this prognostic model. Here, 8 lncRNAs (without MED4-AS1) were utilized for validation since MED4-AS1 expression was not found in NSCLC in this cohort. The results of the survival status scatter plot and heatmap in this cohort were similar to those of the training group (Figure S1A-B, Figure S1 E). K-M analysis illustrated that the risk score based on these 8 lncRNAs are correlated with the prognosis of NSCLC (P = 0.016, Figure S1 C), and the ROC curve also demonstrated a good prediction performance of this prognostic signature (AUC = 0.616, Figure S1 D).

Correlation analysis between risk score and clinical characteristics

The potential relationship between risk score and multiple clinical characteristics (age, gender, EGFR mutation, ALK-EML4 rearrangement, stage and TNM stage) was also analyzed in the present study. The results illustrated that risk score was related to gender, stage and T, N stage, among which, male patients and those with higher T and N stage had higher risk (Fig. 8A-H). Further subgroup analysis found that the T stage is correlated with risk score in both LUAD and LUSC, and stages and N stage were found to relate to the LUAD, and M stage showed a relationship with LUSC (Figure S2).

Univariate Cox regression analysis elucidated that risk score, stage, T, N, M stages are the risk factors for the NSCLC prognosis (P < 0.05, Fig. 8I). Additionally, risk score as well as T, N, M stages remain independent risk factors for the OS of NSCLC patients in multivariate Cox regression analysis (P < 0.05, Fig. 8J). Then, a nomogram merging clinicopathological features and the risk scores was constructed to assist clinical prediction of the prognosis of NSCLC patients (Figs. 9A), and a satisfactory agreement between the predicted and observed values at the probabilities of 1-, 3- and 5-year survival was shown in the calibration curve (Figs. 9B). What's more, the ROC curve revealed that the risk score was more accurate in predicting survival in patients with NSCLC than traditional clinical features (Fig. 9C).

Correlation analysis between risk score and immune cell infiltration

Five algorithms, ESTIMATE, ssGSEA, MCP counter, TIMER and CIBERSORT were utilized to evaluate the correlation between risk score and immune cell infiltration in NSCLC and the results were visualized as heatmap (Fig. 10A-E). The expression of ICGs between the two risk groups was further investigated due to the crucial role of checkpoint inhibitor-based immunotherapies in NSCLC. The results showed a substantial difference in the expression of 45 ICGs between the two risk groups (Table S6), and the first 10 ICGs (BTLA, BTN2A2, CD160, CD226, CD27, CD276, CD40LG, CD96, CTLA4, TIGIT) were presented in Fig. 11A. In addition, there are 8 m6A-related mRNA differentially expressed in the two-risk group, among which, 7 m6A-related mRNAs (ELAVL1、FMR1、IGF2BP1、METTL3、RBM15、YTHDC1, YTHDC2) were highly expressed in the low-risk group, and HNRNPA2B1 was upregulated in the high-risk group (Fig. 11B).

Correlation analysis between risk score and chemotherapeutics sensitivity

As shown in Fig. 12, 28 chemotherapeutics were found to be significantly correlated with the risk score, among which the sensitivity of 19 drugs and the resistance of 9 drugs were significantly correlated with the risk score.

Discussion

Lung cancer, the most fatal malignancy worldwide, has a variety of histological subtypes. As the most prevalent pathological pattern of lung cancer, NSCLC patients are usually diagnosed at an advanced stage with poor survival due to the lack of early specific clinical manifestations, diagnostic and prognostic biomarkers[22]. Over the past decade, the long-term survival rate of advanced NSCLC has been significantly prolonged due to the development of targeted therapies and immunotherapy. Unfortunately, poor prognoses remain in some patients after systemic and targeted therapy [23, 24]. Hence, there is an urgent need for safe and feasible markers that can accurately predict prognosis, so as to make the management of NSCLC patients more accurate, personalized and timely.

Ferroptosis is a newly type regulatory cell death with specific properties and recognizing functions that participated in numerous diseases including cancers [25],which was identified involved in killing malignant cells and inhibiting tumor progression in several cancers, such as NSCLC[26], pancreatic cancer[27], breast cancer [28]and hepatocellular carcinoma[29] and consequently considered as a novel therapeutic strategy for cancer treatment. Interestingly, the crucial role of lncRNAs in the regulation of ferroptosis has been increasingly recognized [30]. Whereas, the role of FRGs-lncRNAs in prognostic, immune response, and chemotherapeutic effect in NSCLC remains unclear.

Herein, the data of LUAD and LUSC from the TCGA database were combined as a matrix of NSCLC for analysis for the first time. We found 59 FRGs and 129 FRGs-lncRNAs differentially expressed between NSCLC and normal patients. Then, 10 FRGs-lncRNAs associated with the OS of NSCLC were further identified. Subsequently, a prognostic model was established in the training set based on the 9 prognostic FRGs-lncRNAs and verified in the internal and external cohort. Additionally, the relationship between risk score and clinical characteristics of NSCLC were assessed and a nomogram was constructed. Finally, the correlation between immune cell infiltration, chemotherapeutic sensitivity as well as risk score were investigated to evaluate the potential role of FRGs-lncRNAs in the immune response and chemotherapeutic effect in NSCLC. These findings strongly suggest a potentially important role of FRGs-lncRNAs in NSCLC.

In our study, the predictive model was established based on the 9 FRGs-lncRNAs (AQP4-AS1, DANCR, LINC00460, LINC00892, LINC00996, MED4-AS1, SNHG7, UCA1, and WWC2-AS2). Aquaporin 4 antisense RNA 1 (AQP4-AS1) transcribes a lncRNA with unknown function, which was found related to the risk of gastric [31] and breast cancer[32]. We found that AQP4-AS1 act as a protector factor in NSCLC. Whereas,

the biological function of AQP4-AS1 in ferroptosis and lung cancer has not been systematically analyzed, which need to be further studied. LncRNA differentiation antagonizing non-protein-coding RNA (DANCR), located on chr.4, is known to suppress epidermal progenitor cell differentiation [33]. Importantly, DANCR was identified to be overexpressed in multiple cancers, promotes malignant biological behavior cancer and chemo-resistance[34]. DANCR was also found upregulated and correlated with the poor prognosis in NSCLC, and which promote the malignancy of NSCLC thorough DANCR/miR-138/Sox4 positive feedback loop[35]. Here, we found that DANCR was a protective factor in NSCLC. LINC00460 was also demonstrated overexpressed in NSCLC and promotes epithelial-mesenchymal transition and cell migration[36], what's more, as an FRGs-lncRNA, LINC00460 was identified as a predictor and potential therapeutic target for EGFR-TKI resistance in NSCLC[37]. Although similar results with the previous studies were found in our study, whether ferroptosis involved in the drug resistance and development of NSCLC needs to be further investigated. Despite several kinds of research that have illuminated the role of LINC00892 and LINC00996 in multiple cancers, their function in NSCLC has not been studied and deserves further investigation considering its significant prognostic value in NSCLC. MED4-AS1 is a novel lncRNA that upregulated in NSCLC and positively associated with poor differentiation and metastasis[38], whereas, MED4-AS1 was identified as a protective factor for OS of NSCLC in the present study. The lncRNA small nucleolar RNA host gene 7 (SNHG7) was considered as an oncogenic lncRNA in NSCLC, hepatocellular carcinoma, breast cancer, and colorectal cancer[39, 40], which was found to modulate malignant character in LUAD through SNHG7/miRNA-181/cbx7 pathway, and mediates cisplatin-resistance in NSCLC through activating PI3K/AKT pathway[41]. Notably, the protective role of lncRNA SNHG7 was revealed in our study. Urothelial carcinoma-associated 1 (UCA1) was found to promote gefitinib-resistance in NSCLC[42], knockdown of UCA1 can impair cell proliferation and promoted the gefitinib-induced cell apoptosis, which was considered as a promising therapeutic target for the NSCLC patients with $EGFR^{+}$ [42]. So far, no studies have been conducted on the biological function of WWC2-AS2 in NSCLC, which needs a systematic study further.

It is worth noting that there are few studies investigating the relationship between ICGs and ferroptosis currently. We found different expression levels of BTLA, BTN2AA2, CD160, CD226, CD27, CD276, CD40LG, CD96, CTLA4, TIGIT between the two risk groups of patients with NSCLC. Of note, the risk score was also demonstrated correlated with the chemotherapeutic effect. These results indicated that these FRGs-lncRNAs may regulate the development and progression of NSCLC by modulating the immune response and play a crucial role in the drug resistance in NSCLC.

The advantage of this study is that the data of LUAD and LUSC were systematically combined for the analysis and an FRGs-lncRNAs prognostic model of NSCLC was constructed for the first time and verified both in an internal and external cohort. What's more, the FRGs-lncRNAs were comprehensively identified both in the TCGA database and LncTarD database. Notably, the association between risk score and chemotherapeutics sensitivity was first analyzed in the present study. However, a prospective cohort and molecular biology experiment need to be conducted to further verify the accuracy of the prognostic model and the function of these FRGs-lncRNAs due to the lack of experimental verification in the present study.

Conclusion

In conclusion, 10 FRGs-lncRNAs associated with the OS of NSCLC were identified and a novel FRGs-lncRNAs prognostic model was constructed in the present study and verified both in the internal and external cohort. Then, the relationship between immune response, chemotherapeutics effectiveness and risk score were further evaluated. These findings have potential reference value for guiding the treatment and prognosis evaluation of NSCLC patients.

Abbreviations

NSCLC: Non-small cell lung cancer; FRGs: ferroptosis-related genes; lncRNAs: LUAD: lung adenocarcinoma; OS: overall survival; LUSC: lung squamous cell carcinoma; TCGA: the Cancer Genome Atlas; m6A: N6-methyladenosne; DE-FRGs: Differentially expressed FRGs; FRG-lncRNAs, FRGs-related lncRNAs; GO: Gene Ontology; KEGG: Kyoto Encyclopedia of Genes and Genomes; K-M: Kaplan–Meier plotter; ROC: receiver operational characteristic; ICGs: immune checkpoint genes; CGP: the Cancer Genome Projec database; AQP4-AS1: Aquaporin 4 antisense RNA 1; DANCR: differentiation antagonizing non-protein-coding RNA; SNHG7: small nucleolar RNA host gene 7; UCA1: urothelial carcinoma-associated 1.

Declarations

ETHICS APPROVAL AND CONSENT TO PARTICIPATE

No ethics committee approval and informed consent of patients were required in this study since the data were obtained from a public database.

CONSENT FOR PUBLICATION

Not applicable.

AVAILABILITY OF DATA MATERIALS

The data of this study were obtained from the publicly available database (https://xena.ucsc.edu/).

COMPETING INTERSETS

The authors declare that they have no competing interests.

FUNDING

This work was funded by the National Natural Science Foundation of China (No. 81802291; to Puyu Shi); Key Research and Development Project of Science and Technology of Shaanxi Province (No. 2018KW-039; to Puyu Shi; No. 2018SF-071; to Hui Ren); Fundamental Research Funds for the Central Universities

in Xi’an Jiaotong University (No. 1191320149; to Puyu Shi); China Postdoctoral Science Foundation Grant (No. 2019M653666; to Puyu Shi).

AUTHOR’ CONTRIBUTION

Conception and design: P Shi, M Chen, M Li; Administrative support: P Shi, M Chen; Data collection and assembly of data: M Li, Y Zhang, M Fan, H Ren; Data analysis and interpretation: M Li, Y Zhang, M Fan, H Ren, P Shi, M Chen; Manuscript writing: All authors; Final approval of manuscript: All authors.

ACKNOWLEDGEMENT

Not applicable.

References

1. Siegel RL, Miller KD, Jemal A. Cancer statistics, 2019. CA Cancer J Clin. 2019; 69: 7–34.

2. Cheng TY, Cramb SM, Baade PD, Youlden DR, Nwogu C, Reid ME. The International Epidemiology of Lung Cancer: Latest Trends, Disparities, and Tumor Characteristics. Journal of thoracic oncology : official publication of the International Association for the Study of Lung Cancer. 2016; 11: 1653-71.

3. de Groot PM, Wu CC, Carter BW, Munden RF. The epidemiology of lung cancer. Transl Lung Cancer Res. 2018; 7: 220 – 33.

4. Qiao M, Jiang T, Liu X, Mao S, Zhou F, Li X, et al. Immune checkpoint inhibitors in EGFR-mutated non-small cell lung cancer: Dusk or Dawn? J Thorac Oncol. 2021.

5. Doroshow DB, Sanmamed MF, Hastings K, Politi K, Rimm DL, Chen L, et al. Immunotherapy in Non-Small Cell Lung Cancer: Facts and Hopes. Clin Cancer Res. 2019; 25: 4592 – 602.

6. Ruiz-Cordero R, Devine WP. Targeted Therapy and Checkpoint Immunotherapy in Lung Cancer. Surg Pathol Clin. 2020; 13: 17–33.

7. Tang D, Chen X, Kang R, Kroemer G. Ferroptosis: molecular mechanisms and health implications. Cell Res. 2021; 31: 107 – 25.

8. Stockwell BR, Friedmann Angeli JP, Bayir H, Bush AI, Conrad M, Dixon SJ, et al. Ferroptosis: A Regulated Cell Death Nexus Linking Metabolism, Redox Biology, and Disease. Cell. 2017; 171: 273 – 85.

9. Xu G, Wang H, Li X, Huang R, Luo L. Recent progress on targeting ferroptosis for cancer therapy. Biochem Pharmacol. 2021: 114584.

10. Shi X, Sun M, Liu H, Yao Y, Song Y. Long non-coding RNAs: a new frontier in the study of human diseases. Cancer Lett. 2013; 339: 159 – 66.

11. Chen Y, Zitello E, Guo R, Deng Y. The function of LncRNAs and their role in the prediction, diagnosis, and prognosis of lung cancer. Clin Transl Med. 2021; 11: e367.

12. Jiang N, Zhang X, Gu X, Li X, Shang L. Progress in understanding the role of lncRNA in programmed cell death. Cell Death Discov. 2021; 7: 30.

13. Wang M, Mao C, Ouyang L, Liu Y, Lai W, Liu N, et al. Long noncoding RNA LINC00336 inhibits ferroptosis in lung cancer by functioning as a competing endogenous RNA. Cell Death Differ. 2019; 26: 2329-43.

14. Gai C, Liu C, Wu X, Yu M, Zheng J, Zhang W, et al. MT1DP loaded by folate-modified liposomes sensitizes erastin-induced ferroptosis via regulating miR-365a-3p/NRF2 axis in non-small cell lung cancer cells. Cell Death Dis. 2020; 11: 751.

15. Mao C, Wang X, Liu Y, Wang M, Yan B, Jiang Y, et al. A G3BP1-Interacting lncRNA Promotes Ferroptosis and Apoptosis in Cancer via Nuclear Sequestration of p53. Cancer Res. 2018; 78: 3484-96.

16. Zhou N, Bao J. FerrDb: a manually curated resource for regulators and markers of ferroptosis and ferroptosis-disease associations. Database (Oxford). 2020; 2020.

17. Zhou Y, Zhou B, Pache L, Chang M, Khodabakhshi AH, Tanaseichuk O, et al. Metascape provides a biologist-oriented resource for the analysis of systems-level datasets. Nat Commun. 2019; 10: 1523.

18. Zhao H, Shi J, Zhang Y, Xie A, Yu L, Zhang C, et al. LncTarD: a manually-curated database of experimentally-supported functional lncRNA-target regulations in human diseases. Nucleic Acids Res. 2020; 48: D118-d26.

19. Tibshirani R. The lasso method for variable selection in the Cox model. Stat Med. 1997; 16: 385 – 95.

20. Simon N, Friedman J, Hastie T, Tibshirani R. Regularization Paths for Cox's Proportional Hazards Model via Coordinate Descent. J Stat Softw. 2011; 39: 1–13.

21. Geeleher P, Cox NJ, Huang RS. Clinical drug response can be predicted using baseline gene expression levels and in vitro drug sensitivity in cell lines. Genome Biol. 2014; 15: R47.

22. Molina JR, Yang P, Cassivi SD, Schild SE, Adjei AA. Non-small cell lung cancer: epidemiology, risk factors, treatment, and survivorship. Mayo Clin Proc. 2008; 83: 584 – 94.

23. Camidge DR, Doebele RC, Kerr KM. Comparing and contrasting predictive biomarkers for immunotherapy and targeted therapy of NSCLC. Nat Rev Clin Oncol. 2019; 16: 341 – 55.

24. Herbst RS, Morgensztern D, Boshoff C. The biology and management of non-small cell lung cancer. Nature. 2018; 553: 446 – 54.

25. Mou Y, Wang J, Wu J, He D, Zhang C, Duan C, et al. Ferroptosis, a new form of cell death: opportunities and challenges in cancer. J Hematol Oncol. 2019; 12: 34.

26. Guo J, Xu B, Han Q, Zhou H, Xia Y, Gong C, et al. Ferroptosis: A Novel Anti-tumor Action for Cisplatin. Cancer Res Treat. 2018; 50: 445 – 60.

27. Yamaguchi Y, Kasukabe T, Kumakura S. Piperlongumine rapidly induces the death of human pancreatic cancer cells mainly through the induction of ferroptosis. Int J Oncol. 2018; 52: 1011-22.

28. Ma S, Henson ES, Chen Y, Gibson SB. Ferroptosis is induced following siramesine and lapatinib treatment of breast cancer cells. Cell Death Dis. 2016; 7: e2307.

29. Sun X, Ou Z, Chen R, Niu X, Chen D, Kang R, et al. Activation of the p62-Keap1-NRF2 pathway protects against ferroptosis in hepatocellular carcinoma cells. Hepatology. 2016; 63: 173 – 84.

30. Xie B, Guo Y. Molecular mechanism of cell ferroptosis and research progress in regulation of ferroptosis by noncoding RNAs in tumor cells. Cell Death Discov. 2021; 7: 101.

31. Xing C, Cai Z, Gong J, Zhou J, Xu J, Guo F. Identification of Potential Biomarkers Involved in Gastric Cancer Through Integrated Analysis of Non-Coding RNA Associated Competing Endogenous RNAs Network. Clin Lab. 2018; 64: 1661-9.

32. Marchi RD, Mathias C, Reiter GAK, Lima RS, Kuroda F, Urban CA, et al. Association between SNP rs527616 in lncRNA AQP4-AS1 and susceptibility to breast cancer in a southern Brazilian population. Genet Mol Biol. 2021; 44: e20200216.

33. Kretz M, Webster DE, Flockhart RJ, Lee CS, Zehnder A, Lopez-Pajares V, et al. Suppression of progenitor differentiation requires the long noncoding RNA ANCR. Genes Dev. 2012; 26: 338 – 43.

34. Jin SJ, Jin MZ, Xia BR, Jin WL. Long Non-coding RNA DANCR as an Emerging Therapeutic Target in Human Cancers. Front Oncol. 2019; 9: 1225.

35. Bai Y, Zhang G, Chu H, Li P, Li J. The positive feedback loop of lncRNA DANCR/miR-138/Sox4 facilitates malignancy in non-small cell lung cancer. Am J Cancer Res. 2019; 9: 270 – 84.

36. Li K, Sun D, Gou Q, Ke X, Gong Y, Zuo Y, et al. Long non-coding RNA linc00460 promotes epithelial-mesenchymal transition and cell migration in lung cancer cells. Cancer Lett. 2018; 420: 80–90.

37. Nakano Y, Isobe K, Kobayashi H, Kaburaki K, Isshiki T, Sakamoto S, et al. Clinical importance of long non-coding RNA LINC00460 expression in EGFR-mutant lung adenocarcinoma. Int J Oncol. 2020; 56: 243 – 57.

38. Wang XW, Guo QQ, Wei Y, Ren KM, Zheng FS, Tang J, et al. Construction of a competing endogenous RNA network using differentially expressed lncRNAs, miRNAs and mRNAs in non-small cell lung cancer. Oncol Rep. 2019; 42: 2402-15.

39. Pei YF, He Y, Hu LZ, Zhou B, Xu HY, Liu XQ. The Crosstalk between lncRNA-SNHG7/miRNA-181/cbx7 Modulates Malignant Character in Lung Adenocarcinoma. Am J Pathol. 2020; 190: 1343-54.

40. Shan Y, Ma J, Pan Y, Hu J, Liu B, Jia L. LncRNA SNHG7 sponges miR-216b to promote proliferation and liver metastasis of colorectal cancer through upregulating GALNT1. Cell Death Dis. 2018; 9: 722.

41. Chen K, Abuduwufuer A, Zhang H, Luo L, Suotesiyali M, Zou Y. SNHG7 mediates cisplatin-resistance in non-small cell lung cancer by activating PI3K/AKT pathway. Eur Rev Med Pharmacol Sci. 2019; 23: 6935-43.

42. Chen X, Wang Z, Tong F, Dong X, Wu G, Zhang R. lncRNA UCA1 Promotes Gefitinib Resistance as a ceRNA to Target FOSL2 by Sponging miR-143 in Non-small Cell Lung Cancer. Mol Ther Nucleic Acids. 2020; 19: 643 – 53.

Figures

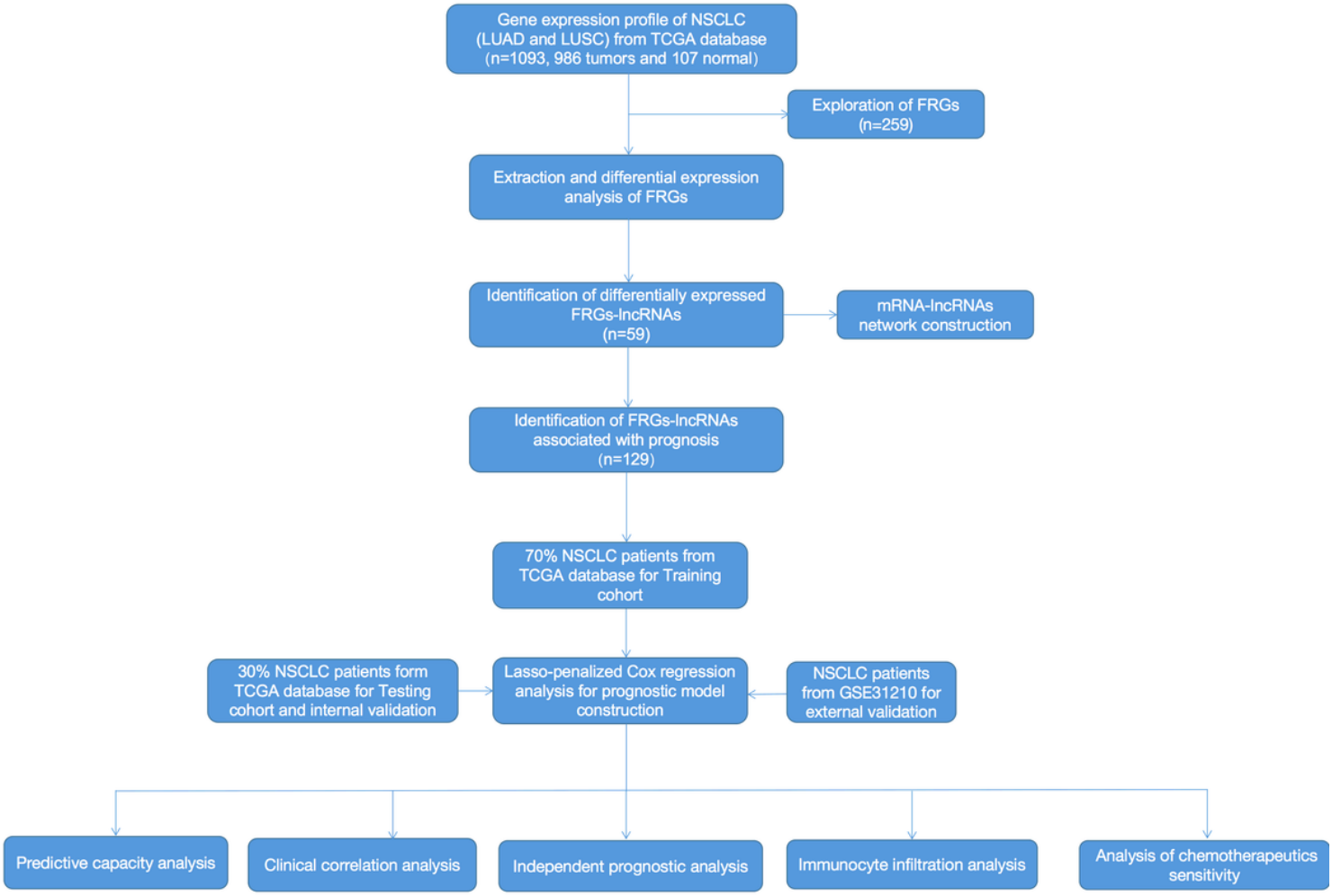

Figure 1

Flowchart of the present study.

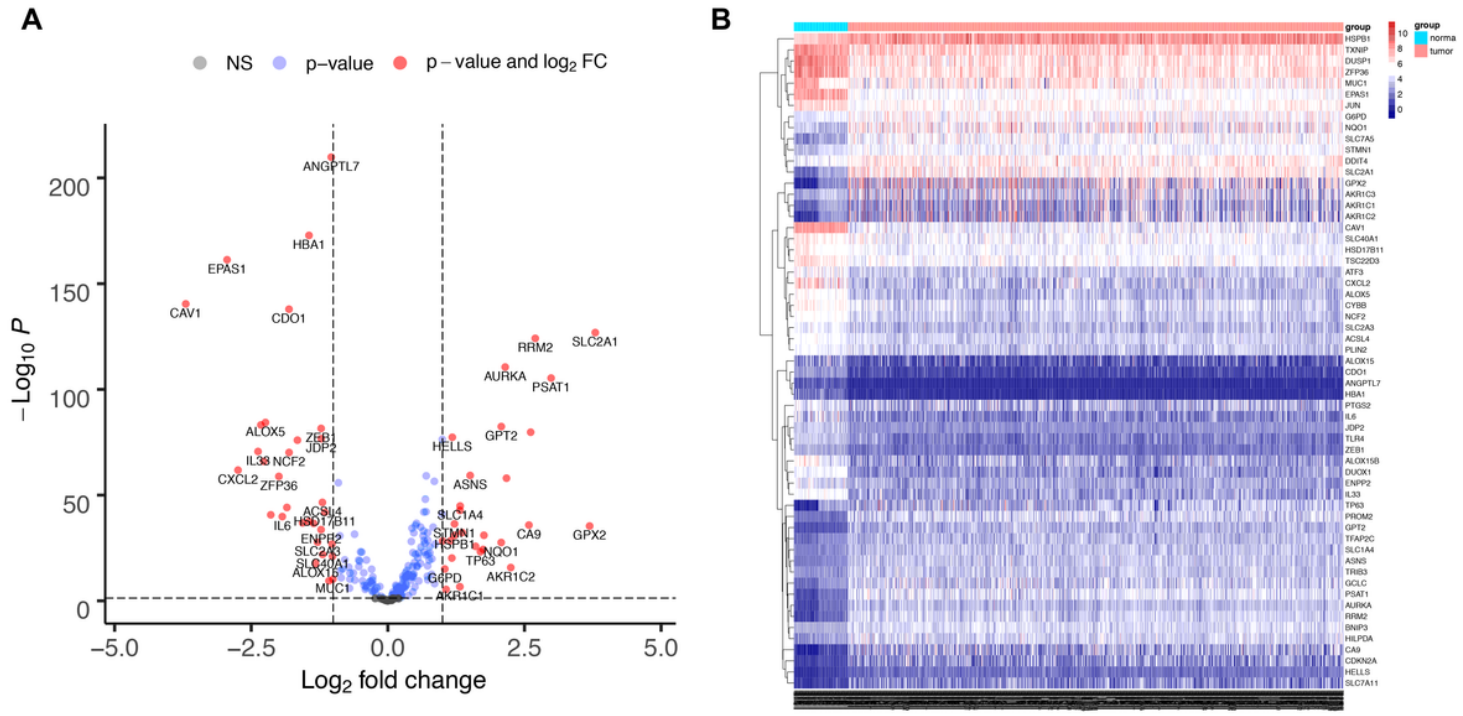

Figure 2

Identification of the FRGs in patients with NSCLC. The DE-FRGs in NSCLC were shown in the volcano plot (A) and heatmap (B). FDR<0.05 and |log2FC|≥1 were considered significant. FRGs, ferroptosis-related genes; DE-FRGs, differentially expressed FRGs; NSCLC, non-small cell lung cancer.

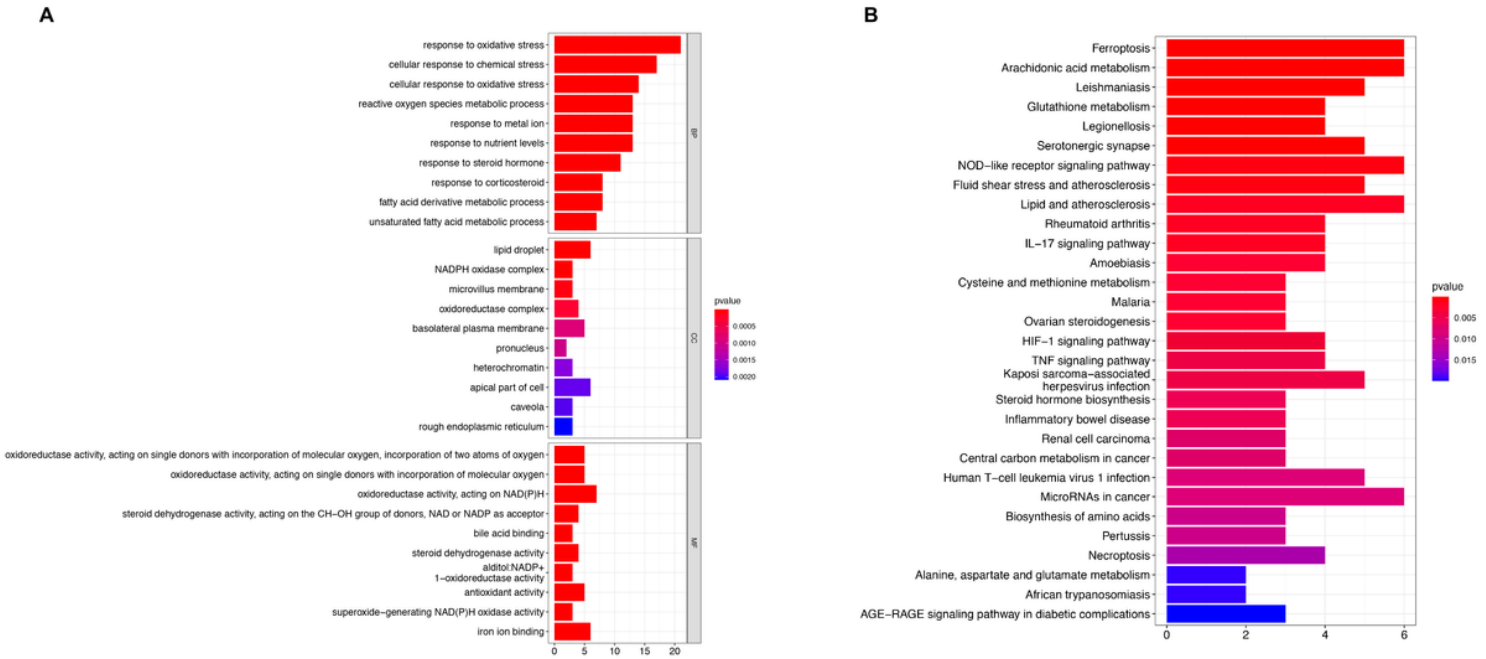

Figure 3

GO (A) and KEGG (B) analysis of the DE-FRGs. GO, Gene Ontology; KEGG, Kyoto Encyclopedia of Genes and Genome; FRGs, ferroptosis-related genes; DE-FRGs, differentially expressed FRGs.

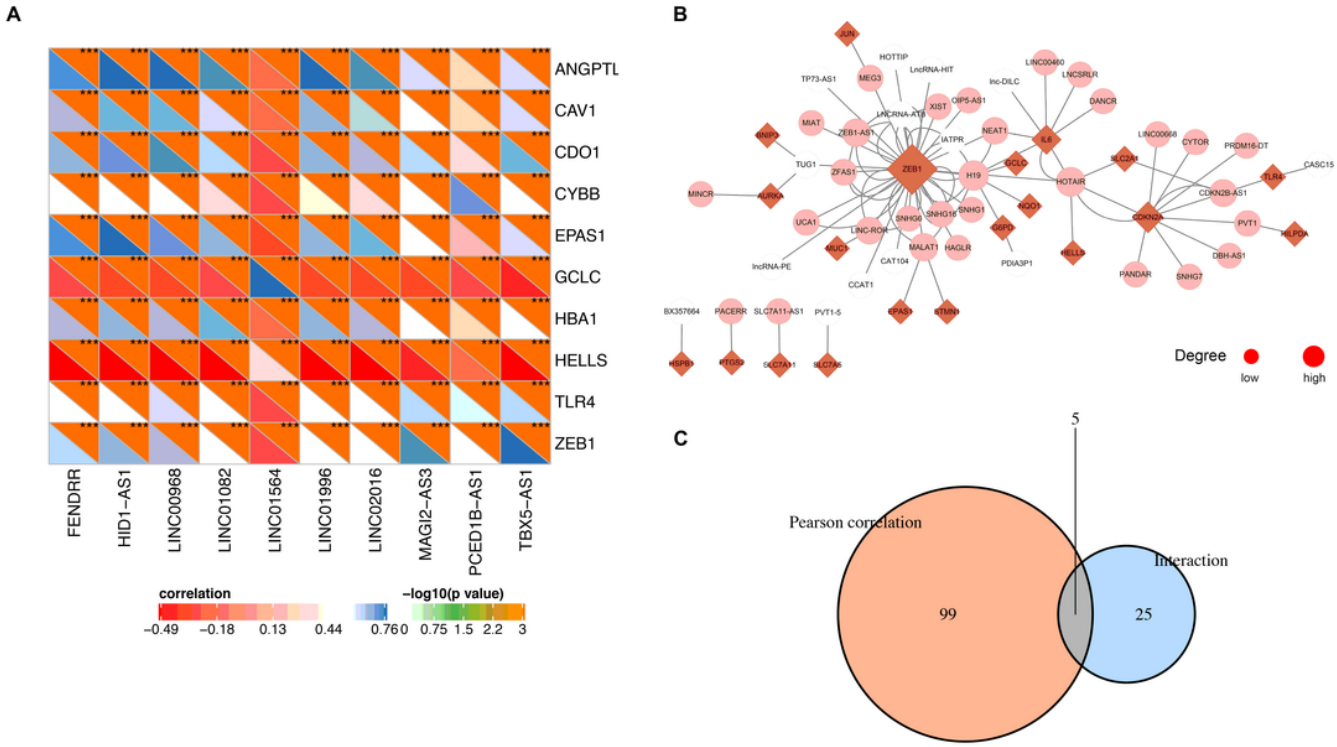

Figure 4

Identification of the FRGs-lncRNAs in NSCLC. (A) Correlation heatmap of the top 10 FRGs and lncRNAs base on TCGA database. The criteria of correlation analysis: |R|>0.5 and P<0.001. (B) Interaction network between DE-FRGs and lncRNAs in LncTarD database. The DE-FRGs and lncRNAs are shown as the red diamond and pink circle, respectively. The white circles represent lncRNAs that are not expressed in NSCLC. The size of the dot is positively correlated with the degree. (C) The union set of the DE-FRGs related lncRNAs in the TCGA database and LncTarD database were shown as a Venn diagram. FRGs, ferroptosis-related genes; lncRNAs: long non-coding RNAs; FRGs-lncRNAs, FRGs-related lncRNAs; TCGA: the Cancer Genome Atlas; NSCLC, non-small cell lung cancer; DE-FRGs: differentially expressed FRGs.

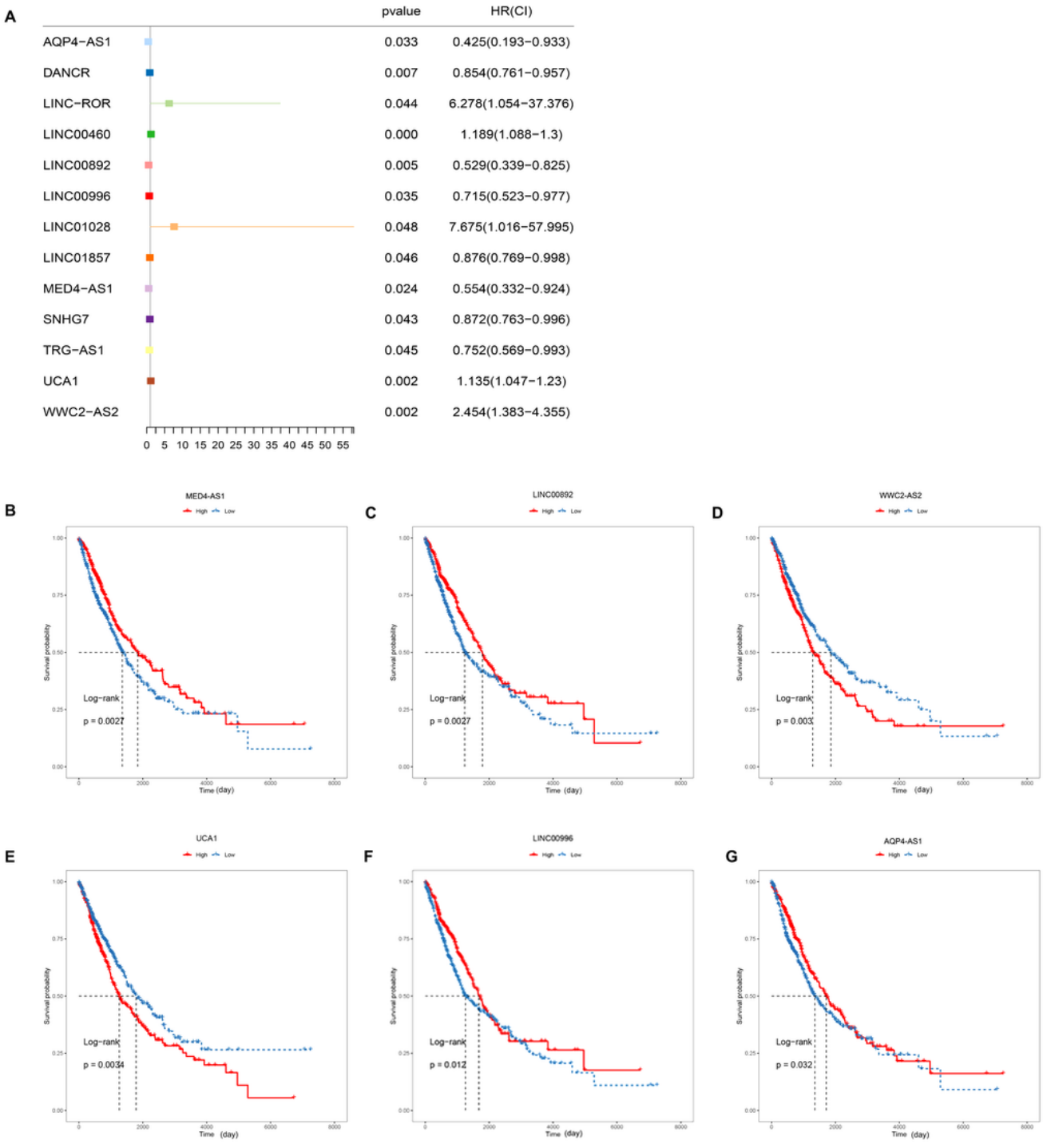

Figure 5

Identification of the FRGs-lncRNAs associated with prognosis. Univariate Cox regression analysis (A) and Kaplan-Meier survival analysis (B-G) identified the FRGs-lncRNAs associated with prognosis of NSCLC. NSCLC, non-small cell lung cancer; FRGs, ferroptosis-related genes; FRGs-lncRNAs: FRGs related lncRNAs.

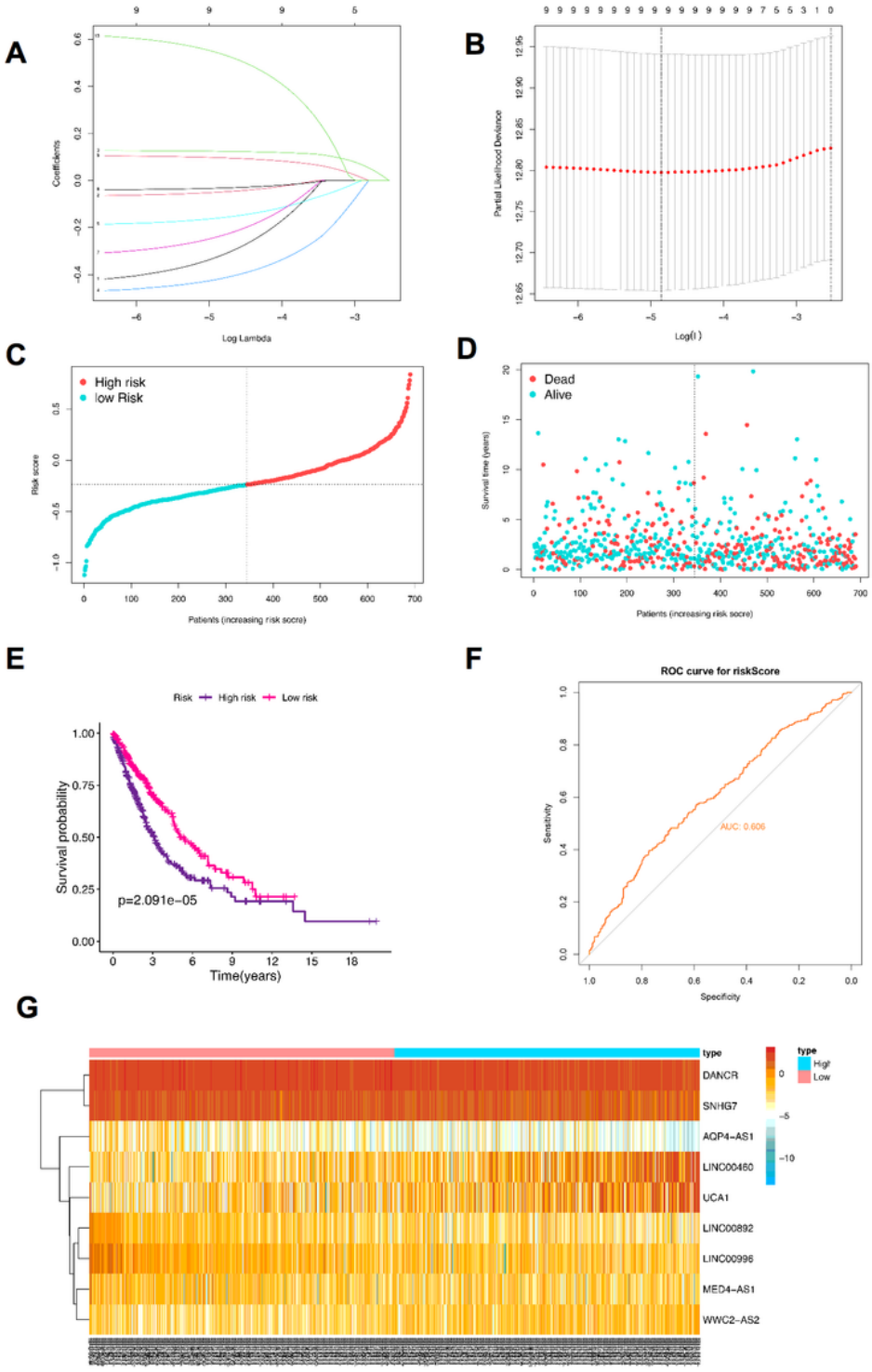

Figure 6

Construction of the FRGs-lncRNAs signature in the training group. (A) Lasso coefficients profiles of the 10 FRGs-lncRNAs. (B) Lasso regression analysis obtained 9 prognostic FRGs-lncRNAs. Distribution (C) and survival status plot (D) of NSCLC patients based on the median risk score. Kaplan-Meier survival (E) and ROC curve analysis (F) of the FRGs-lncRNAs signature in training group. (G) Heatmap of the expression profiles of the FRGs-lncRNAs in low- and high-risk groups. NSCLC, non-small cell lung cancer; lncRNAs:

long non-coding RNAs; FRGs, ferroptosis-related genes; FRGs-lncRNAs: FRGs related lncRNAs; ROC, receiver operating characteristic.

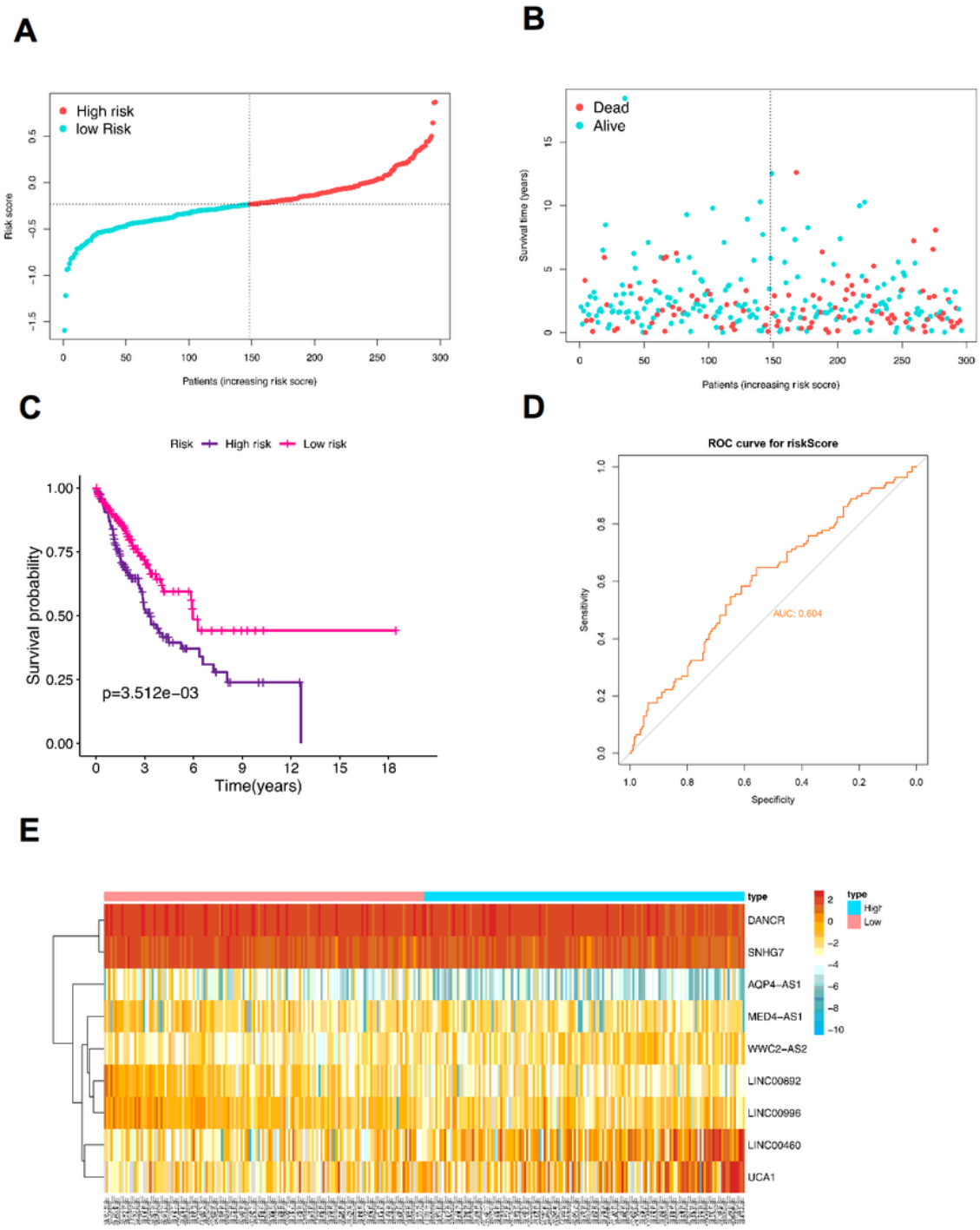

Figure 7

Validation of the FRGs-lncRNAs signature. Distribution (A) and survival status plot (B) of NSCLC patients based on the median risk score. Kaplan-Meier survival (C) and ROC curve analysis (D) of the FRGs-lncRNAs signature in internal testing group. (E) Heatmap of the expression profiles of the FRGs-lncRNAs

in low- and high-risk groups. NSCLC, non-small cell lung cancer; lncRNAs: long non-coding RNAs; FRGs, ferroptosis-related genes; FRGs-lncRNAs: FRGs related lncRNAs; ROC, receiver operating characteristic.

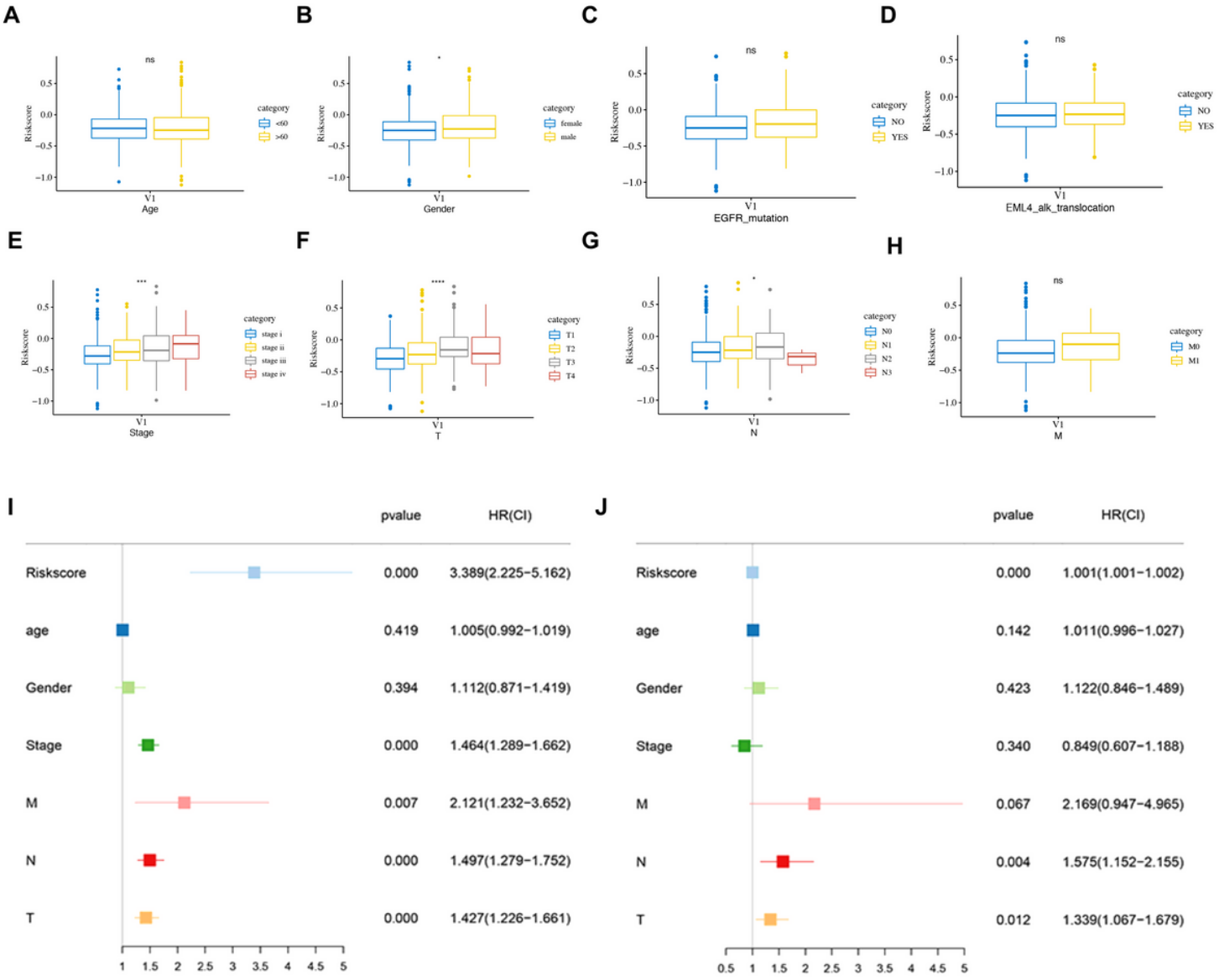

Figure 8

Correlation analysis and independent prognostic analysis. Correlation analysis between risk score and Age (A), Gender (B), EGFR mutation (C), ALK-EML4 rearrangement (D), stage (E), T (F), N (G) M (H) Stage. The univariate (I) and multivariate (J) Cox regression analysis of the associations between the risk score, clinical parameters and OS in NSCLC patients. NSCLC, non-small cell lung cancer; OS, overall survival.

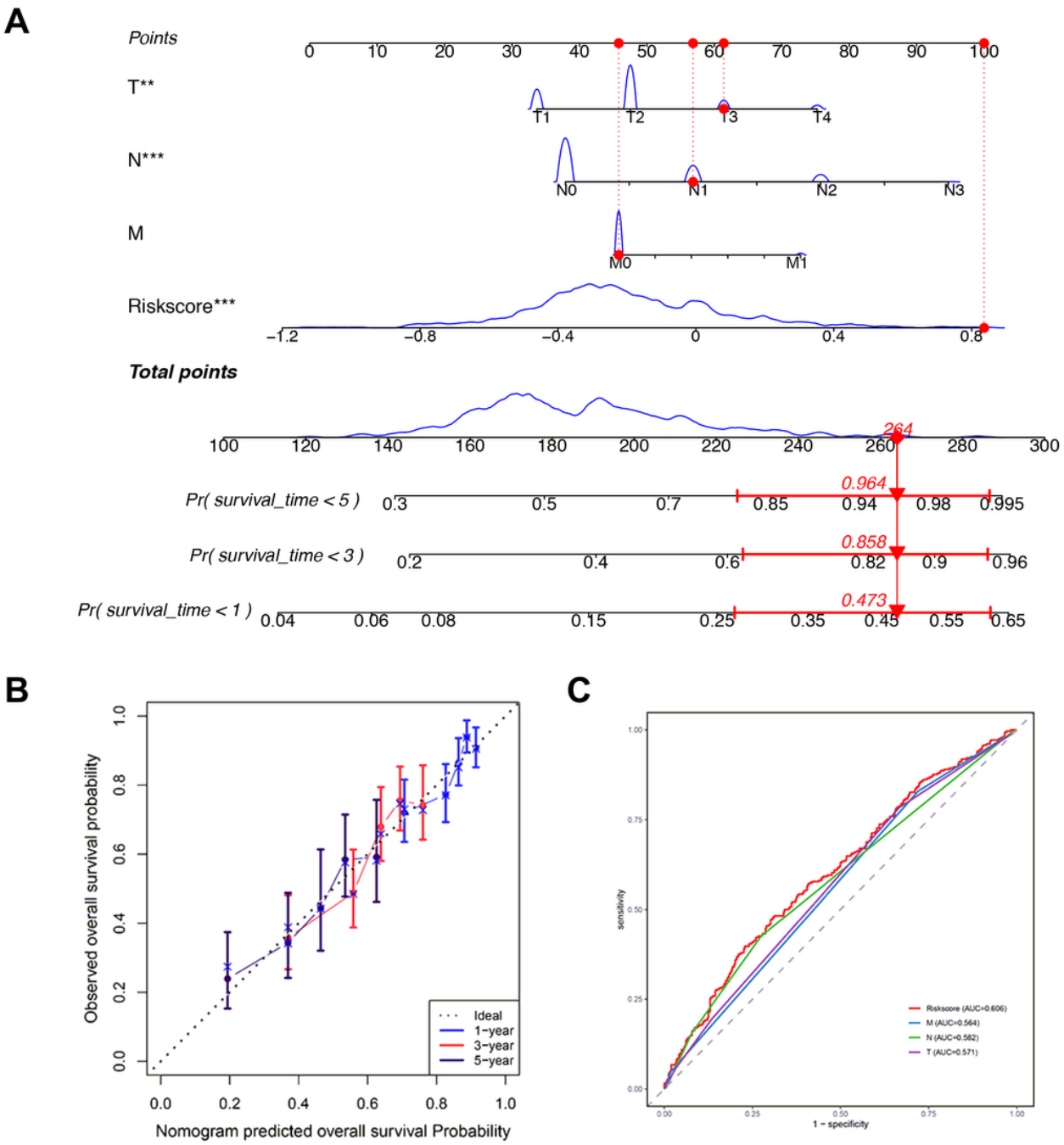

Figure 9

A nomogram construction and evaluation. (A) The nomogram of the prognostic model based on the clinic-pathological factors and FRGs-lncRNAs. (B) The calibration curves of the nomogram for predicting 1-, 3- and 5-years survival of NSCLC patients. (C) ROC curve of clinic-pathological factors and risk score for predicting prognosis of NSCLC. NSCLC, non-small cell lung cancer; OS, overall survival. FRGs, ferroptosis-related genes; FRGs-lncRNAs, FRGs-related lncRNAs; OS, overall survival.

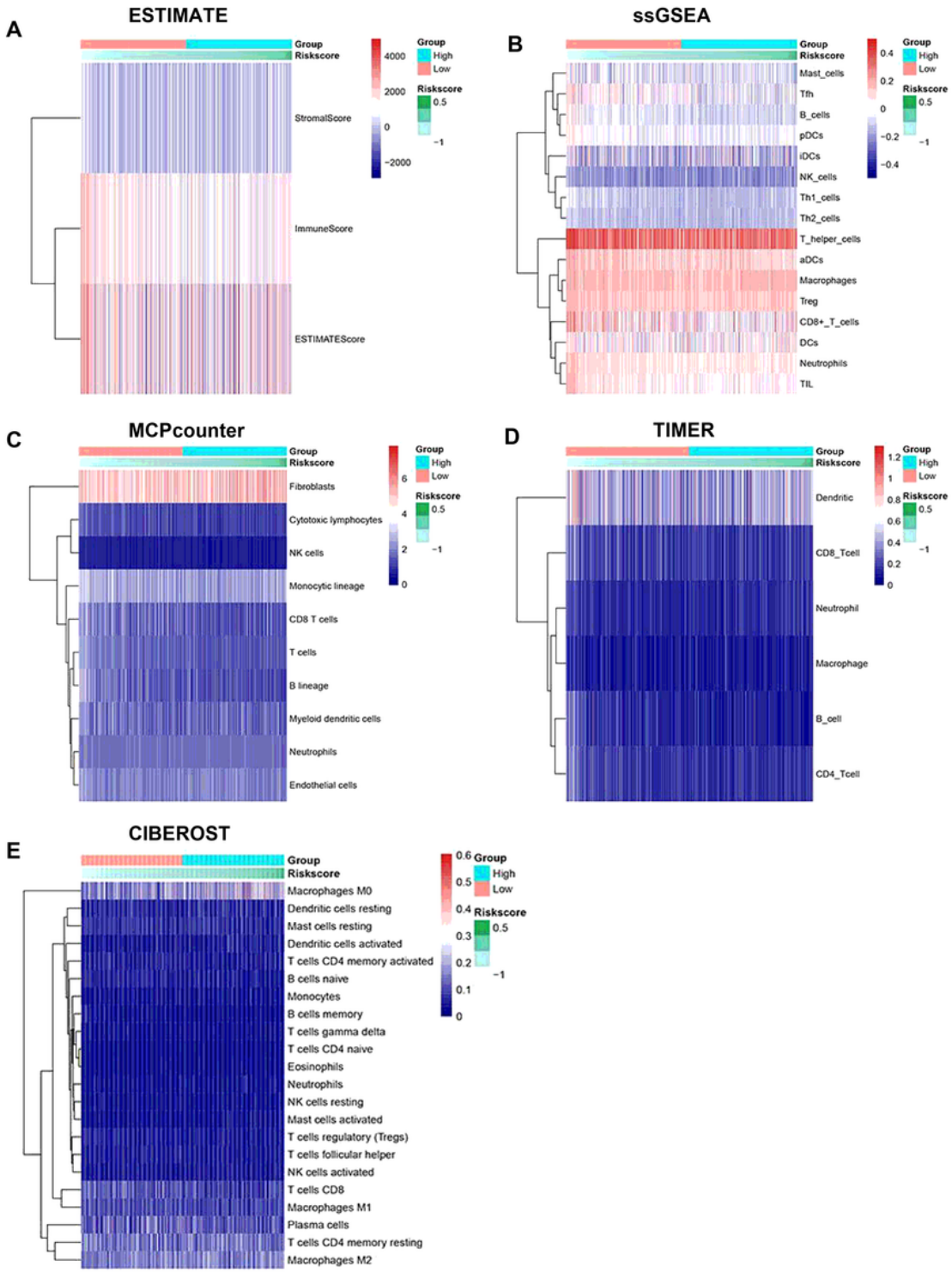

Figure 10

Heatmap for immune responses based on ESTIMATE (A), ssGSEA (B), MCPcounter (C), TIMER (D) and CIBERSORT (E) algorithms among the high and low-risk group.

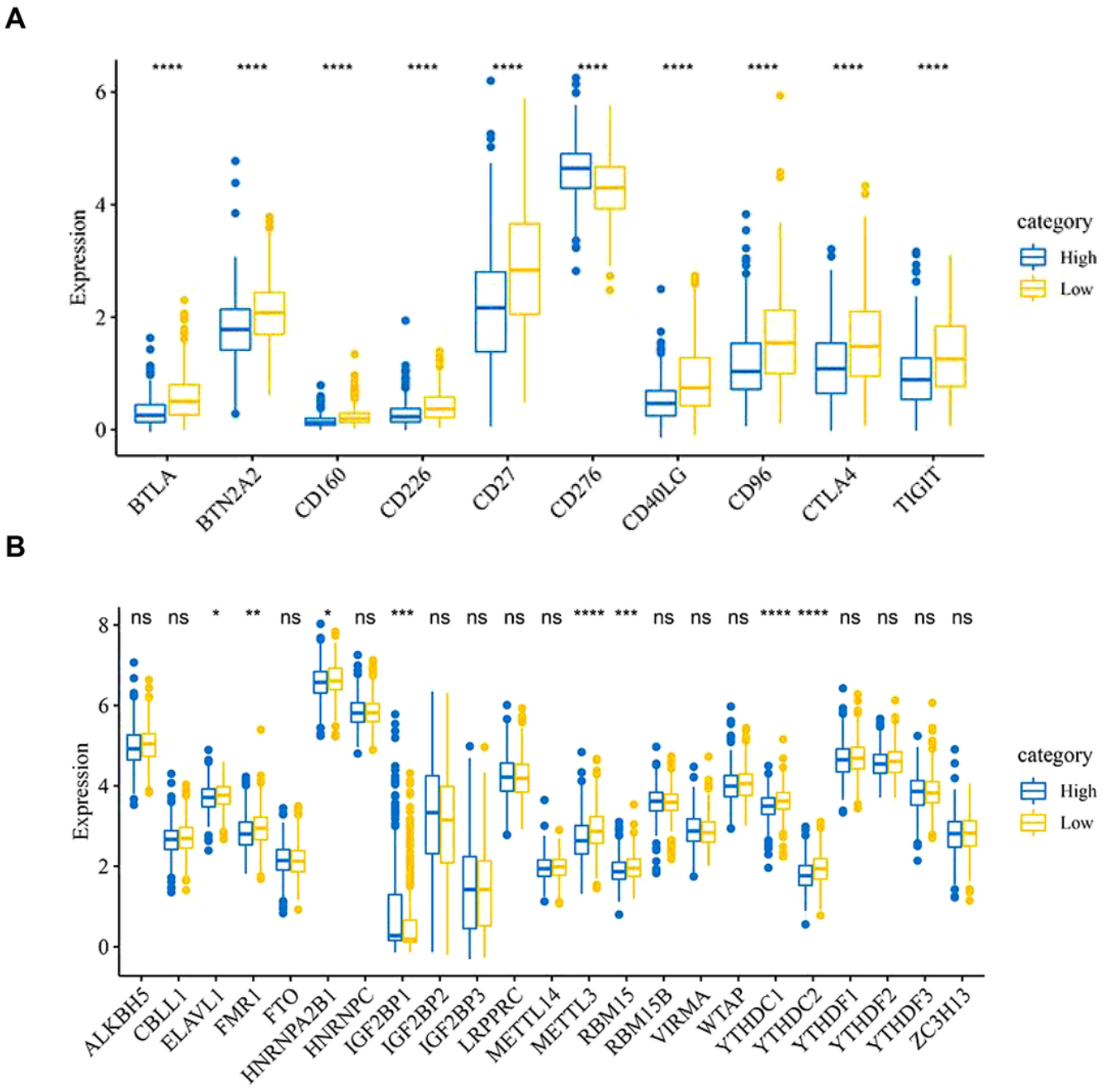

Figure 11

Expression of immune checkpoints (A) and m6A-related genes (B) between high- and low- risk groups of NSCLC. NSCLC, non-small cell lung cancer; m6A: N6-methyladenosne.

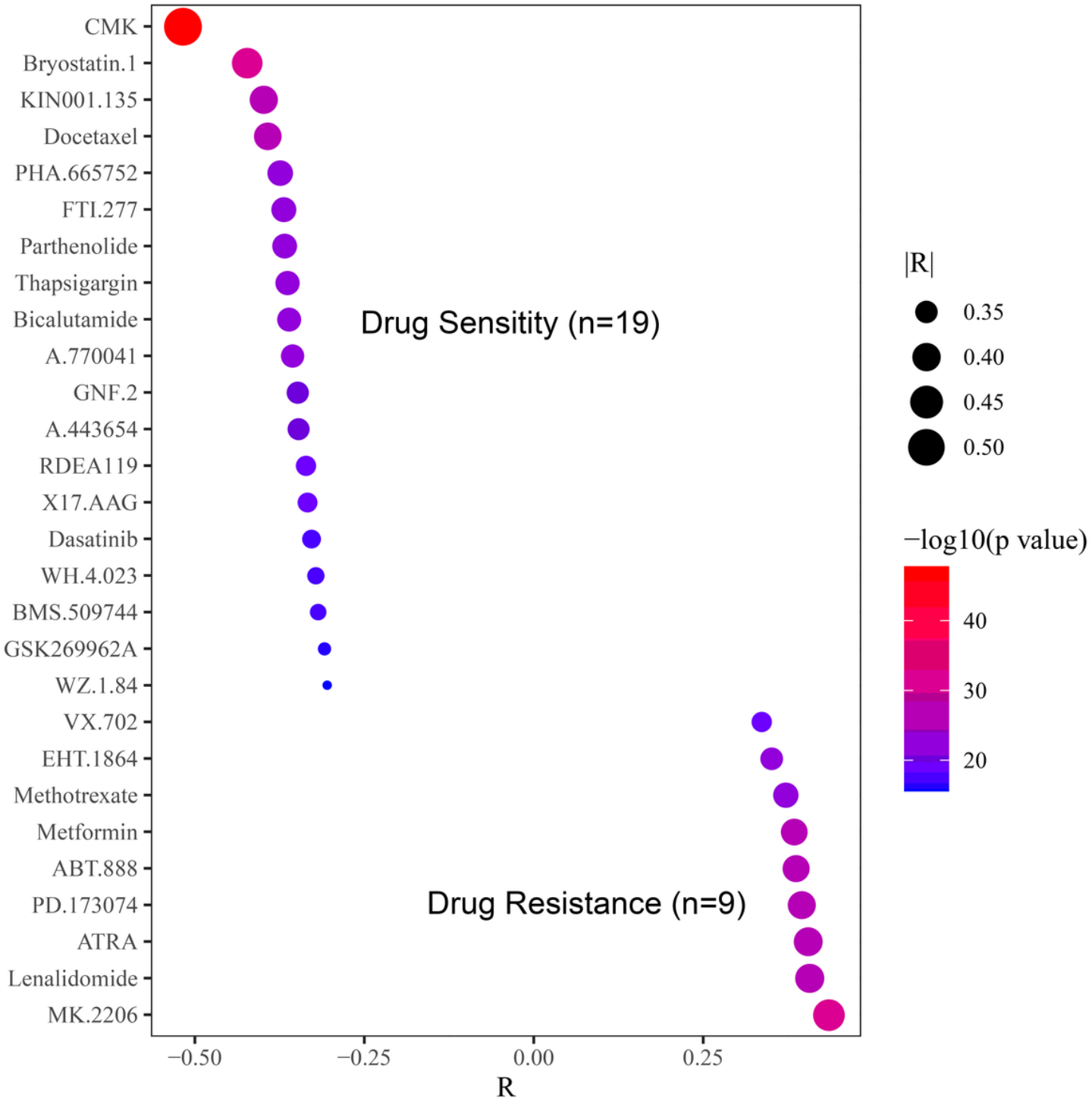

Figure 12

Correlation analysis of risk score and chemotherapeutics sensitivity in NSCLC. NSCLC, non-small cell lung cancer.

Supplementary Files

This is a list of supplementary files associated with this preprint. Click to download.

- figS1.tif
- FigS2.tif
- sTable.xlsx